Quasars, Isotropy of H0 and the local Supercluster of Galaxies

Henri Reboul

Astron. Astrophys. 89, 272–281 (1980)

ASTRONOMY AND ASTROPHYSICS

Quasars, Isotropy of H_0 and the Local Supercluster of Galaxies

H. J. Reboul

Laboratoire d'Astronomie, Université des Sciences et Techniques du Languedoc, F-34060 Montpellier-Cedex, France

Received May 3; accepted December 5, 1979

Summary. A method is described and applied to test the isotropy of H_0 on a sample of quasars ($0.2 \leqq z \leqq 3.5$). Quasars are selected by their radio index ($-\alpha \geqq 0.7$ or $|\alpha| \leqq 0.3$). Generalized Hubble moduli HM* are computed for each object taking into account q_0, colour, galactic extinction and K-correction. HM* is then an individual measure of H_0.

A systematic search for hemispheric anisotropy does not detect departures from isotropy at 50% level of confidence. Upper limits for a possible hemispheric anisotropy of H_0 at very large distances are +34% and −25%. No smaller scale anisotropy is revealed.

Further study seems to show that HM* is minimum through the disk and in the general direction of the centre of the Local Supercluster. This could be a sign of supergalactic extinction. Such an extinction had already been suggested from studies of colour excess of galaxies but is controversial. New studies on our sample show that the dependence of HM* on supergalactic latitude is consistent with supergalactic extinction but no conclusion is drawn because of both the amount of dispersion in the data and the large value (0.8 ± 0.5 mag) which would be needed for this extinction.

Key words: quasars – Hubble Law – local supercluster

Introduction

The isotropy of the redshift-distance relation at low and medium distances and its correlation with the Local Supercluster of Galaxies (LSG) have been widely investigated (Rubin, 1951; de Vaucouleurs, 1958, 1964, 1976, 1977; de Vaucouleurs and Peters, 1968; de Vaucouleurs and Bollinger, 1979).

This problem has been extended to intermediate distances by Rubin et al. (Rubin et al., 1973, 1976) and in other phenomenological interpretations of the observed anisotropy (Jaakola et al., 1975, 1976; Le Denmat and Vigier, 1975; Karoji and Moles, 1975; Karoji and Nottale, 1976; Karoji et al., 1975a, b; Nottale, 1976; Nottale and Vigier, 1977).

The initial aim of the present study is a test of the isotropy of H_0 at very large distances using a population of quasars. At first sight, the high dispersion that quasars show – at least with the hypothesis of the cosmological nature of their redshift – suggests that such a study will be afflicted with great uncertainties and that no significant result will be found. Nevertheless, intrinsic properties of quasars can be used to select much less dispersed samples allowing cosmological statistical studies.

General Method

A simple way to test the isotropy of H_0 in a sample is to define for each object a modulus which acts as a measure of H_0 and then to study the isotropy of this modulus.

A classical Hubble modulus HM has been defined and used by Rubin et al. (1973):

$$\mathrm{HM} = \log(cz) - 0.2\,\mathrm{m} = \log \mathrm{H}_0 - 0.2\,M - 5 \tag{1}$$

where c is the velocity of light, H_0 the Hubble constant, m and M apparent and absolute magnitudes of an object, and z its redshift. This definition is adequate for studies at $z < 0.1$. At larger redshifts, it is necessary to include cosmological models, at least to see if any observed anisotropy is model-dependent.

It has been shown elsewhere (Cordoni and Reboul, 1979) that generalized Hubble moduli could be deduced in the case of Friedmann's models:

$$\begin{aligned}\mathrm{HM}^* &= \log\{cq_0^{-2}\{q_0 z + (q_0 - 1)[(1 + 2q_0 z)^{1/2} - 1]\}\} - 0.2\,m \\ &= \log \mathrm{H}_0 - 0.2\,M - 5.\end{aligned} \tag{2}$$

These HM* offer all the properties of the classical HM, but they require a choice for q_0.

All the following experiments were done with four values for q_0: 0, 0.2, 0.5, and 1. The steady-state Hoyle's model ($q_0 = -1$) for which $\mathrm{HM}^* = \log\{cz(1+z)\} - 0.2\,m$ (3), has been added for comparison.

Hypotheses and Tests

The fundamental hypotheses of the present work are as follows:

(i) the redshifts of quasars are mainly cosmological

(ii) a Friedmann's model is a good first order approximation for the Universe.

The hypotheses to be tested are:

(i) (phenomenological) H_0 is isotropic

(ii) (statistical) HM* is a Gaussian isotropic parameter.

We call $\boldsymbol{H}$ the phenomenological hypothesis and $\boldsymbol{H}'$ the statistical one (our model).

In keeping with the method above, we shall start testing $\neg \boldsymbol{H}'$, i.e., "Is $\boldsymbol{H}'$ wrong?". If we get a negative answer, we will then try to set an upper limit for a possible anisotropy.

There lies the "*a priori*" part of our statistical study. We reserve the opportunity to look at other hypotheses which could match "*a posteriori*" features of our analysis, but without any claim to the objectivity of the first study.

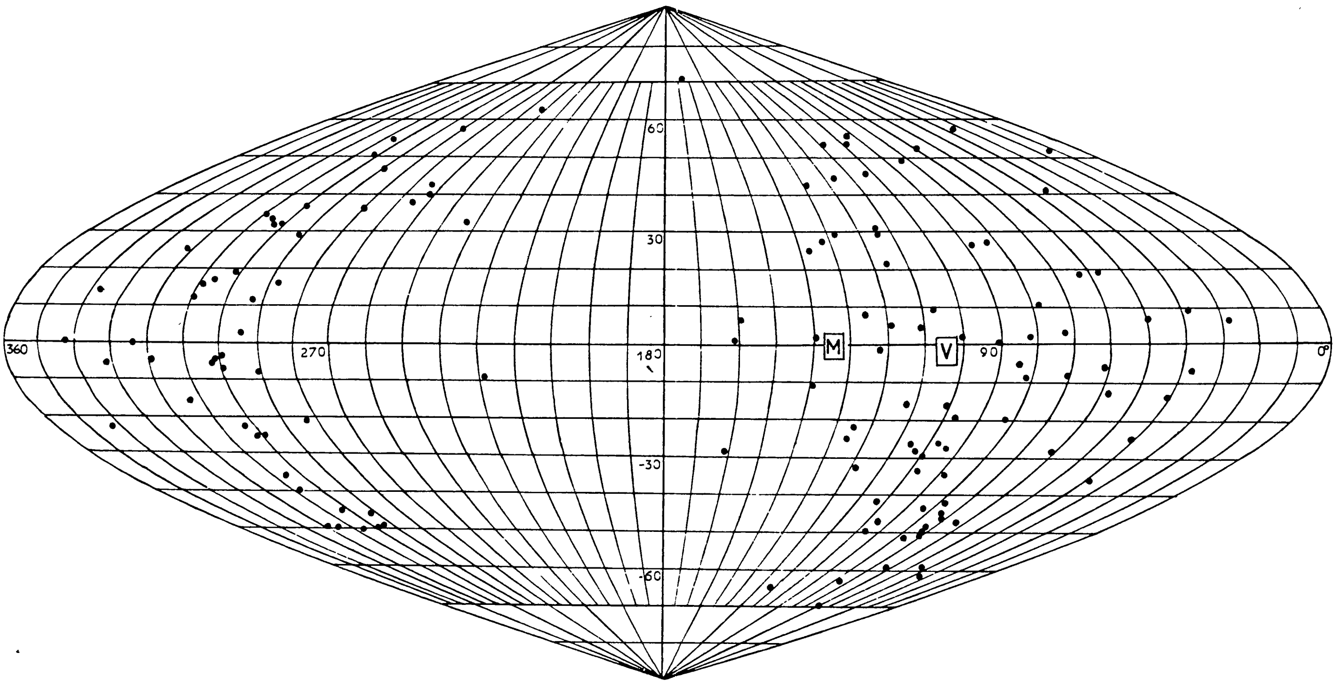

Fig. 1. Distribution in supergalactic coordinates of the 132 quasars selected by their radio spectral index ($-\alpha \geqq 0.7$ or $|\alpha| \leqq 0.3$). The galactic disk is roughly along the central meridian and at the periphery of the chart. Point M gives the position of the extremum (minimum) of ΔHM^* which has been found in the second part of the study. The position of the Virgo cluster is marked as V

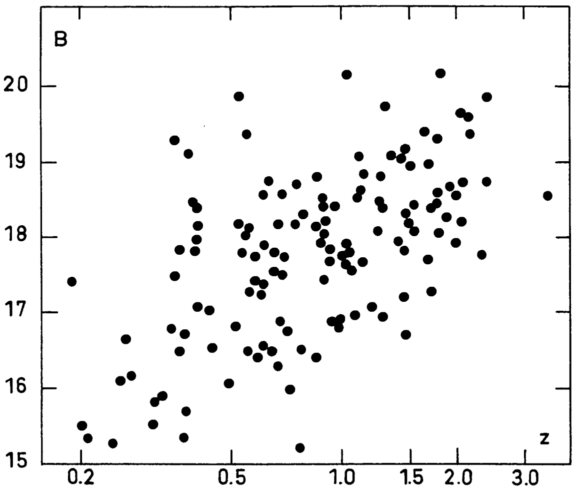

Fig. 2. Hubble diagram of the selected sample. B_0 is the magnitude corrected for colour, galactic extinction, and K-correction. z is the emission redshift. A line of slope 1 (graphical) would depict the classical Hubble law

Sample

Choice

Setti and Woltjer (1973a, b) and Stannard (1973) have shown that quasars selected by means of radio spectral index – namely very steep and very flat spectra – were much less scattered than the global population on a Hubble diagram.

We started with the 403 quasars of the Smith-Haeni's catalogue (Smith-Haeni, 1977) and we selected the 132 objects which matched the condition $-\alpha \geqq 0.7$ or $|\alpha| \leqq 0.3$ where α is the spectral index between 408 and 1415 MHz. The apparent distribution of the selected sample is shown in Fig. 1.

Corrections

Magnitudes were taken from the catalogue of Smith-Haeni and reduced to the B system. When $B-V$ was not available, we applied the standard $B-V$ derived from the redshift, according to Evans and Hart (1977).

We applied the B corrections of galactic extinction according to de Vaucouleurs et al. (1976).

K-corrections for B magnitudes have been made according to Evans and Hart (1977). For $z>2.5$, K_B was computed from the K_U of Evans and Hart through their transformation formula (number 4 in their paper) and by the choice of $U-B=-0.62$ for $z=0$. This leads to

$$K_B(z_B)=K_U(z_U)-0.13 \quad (4)$$

with

$$z_U=(1+z_B)\,(3593/4408)-1. \quad (5)$$

So, we completed the Table 3 of Evans and Hart until $z=3.5$. This extension was necessary because of the strong increase of K_B at $z>2.7$ which reflects the increase of K_U for $z>2$ (Fig. 3c of Evans and Hart's paper).

Solar motion corrections have been omitted since they are negligible. The mean z of our sample is 1.01 and a Sun velocity of 390 km s^{-1} (Smoot et al., 1977) could only produce a correction in HM* in the range $\Delta\,\text{HM}^* \sim (1/2.3)\,(\Delta cz/cz) = 6\;10^{-4}$, i.e., one hundredth of the effect which will be discussed.

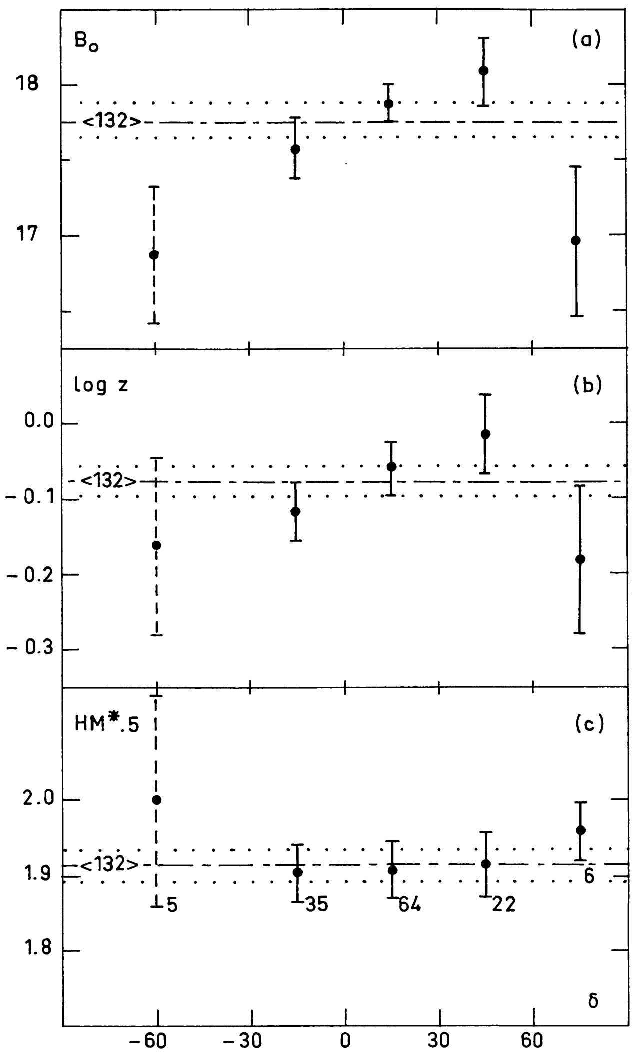

Fig. 3a–c. Selection effects in δ. Standard errors are figured for each mean value. **a** B_0 versus δ: magnitude is correlated with the geographic density of observatories. **b** log z versus δ on a scale consistent with a). **c** HM* 0.5 versus δ: absence of effect shows that effects in (a) and (b) do not bias the present statistics. The number of objects in each zone is indicated. ⟨132⟩ is the total sample

Statistical Properties

Generalized Hubble moduli HM* were computed with corrected *B* magnitude (B_0) and emission redshifts of the 132 quasars, and for the above-mentioned five values of q_0.

The Hubble diagram of the corrected sample is shown in Fig. 2, which indicates a clear Hubble relation.

Statistical properties of the HM* sample are summarized in Table 1. They have been computed for the five values of q_0.

For $q_0=0.5$ and $H_0=100$ km s^{-1} Mpc^{-1}, the mean B_0 magnitude is: -24.56 ± 1.27 (std. deviation). The low values of γ_1 (skewness) and γ_2 (excess) support our model (according to which HM* is a Gaussian parameter). We recall that:

$$\gamma_1=(1/N\sigma^3) \sum_{i=1}^{N} (x_i-\bar{x})^3 \qquad (6)$$

Table 1. Statistical parameters of the HM* sample. ⟨HM*⟩: mean. σ: standard deviation. γ_1: coefficient of skewness. γ_2: coefficient of excess

q_0	HM*	σ	γ_1	γ_2
-1	2.1325	0.3304	-0.0830	-0.2335
0	2.0172	0.2970	-0.1285	-0.0969
0.2	1.9668	0.2737	-0.2267	-0.0556
0.5	1.9126	0.2548	-0.2869	+0.0285
1	1.8484	0.2377	-0.3389	+0.1220

and

$$\gamma_2=(1/N\sigma^4) \sum_{i=1}^{N} (x_i-\bar{x})^4-3 \qquad (7)$$

Working Sample

(See Table 2 and its footnotes).

Selection Bias

A preliminary for the soundness of a study on isotropy is a search for selection bias which may be expected for faint objects.

Figure 3a shows the variation of B_0 (corrected *B* magnitude) versus declination δ. A clear maximum appears at the latitude of the great Northern observatories. Is this selection effect caused by the intrinsic brightness of selected quasars, or is it only reflecting a deeper investigation at $\delta \sim +40°$? Figure 3b shows that the variation of redshift with δ is almost the same and Fig. 3c confirms that there is no effect for HM* versus δ. So, we may think that the selection in δ is more likely to correspond to a deeper spatial study at $\delta \sim +40°$ than to a selection of intrinsically fainter objects and should not cause bias in our work.

Hemispheric Anisotropy

Real Sample

The method of analysis was as follows: we divided the sky into two hemispheres (I and II), we computed the mean HM* in each hemisphere and the difference ΔHM* $=\langle$HM*$\rangle_{\rm I}-\langle$HM*$\rangle_{\rm II}$. Then, the pole of partition (centre of hemisphere I) was rotated in steps of 10° in both supergalactic coordinates, and ΔHM* calculated for the new pole, and so on. We find two extrema of comparable significance: ($q_0=0.5$)

(i) SGL 135°, SGB $-25°$, with ΔHM* $=-0.1051$ and a partition (75,57)

(ii) SGL 135°, SGB $+5°$, with ΔHM* $=-0.1031$ and a partition (72,60).

Results for other values of q_0 are summarized in Table 3. The positions of the extrema are quite unaffected. Intensities differ slightly but are in agreement with the variations of the standard deviation of the sample. Thus, we are going to study the significance of the results above only in the $q_0=0.5$ case.

Table 2. Working sample

a

ALPHA 1	DELTA 2	GL 3	GB 4	SGL 5	SGB 6	Z 7	V 8	B-V 9	B 10	AB 11	KB 12	B0 13	SPI 14	HM*-1 15	HM*0 16	HM*.2 17	HM*.5 18	HM*1 19
0 3 26	15 53 0	107.3	-45.3	309.2	15.8	0.450	16.40	0.11	16.51	0.24	-0.23	16.50	0.70	1.991	1.918	1.896	1.868	1.830
0 3 49	0 21 7	99.8	-60.2	293.0	11.7	1.037	19.40	0.79	20.19	0.21	-0.15	20.13	0.72	1.776	1.649	1.596	1.538	1.467
0 17 50	15 24 17	112.0	-46.5	309.5	12.3	2.012	18.20	0.23	18.43	0.23	-0.32	18.52	1.02	2.555	2.379	2.277	2.180	2.076
0 32 23	42 21 24	119.7	-20.1	337.4	14.2	1.588	18.30	* 0.20	18.50	0.40	-0.28	18.38	0.76	2.416	2.256	2.176	2.094	2.003
0 38 24	-2 3 8	116.7	-65.1	293.8	2.9	1.176	18.50	* 0.35	18.85	0.20	-0.13	18.78	0.73	2.128	1.992	1.932	1.867	1.791
1 6 4	1 19 2	131.8	-61.0	298.9	-2.8	2.107	18.40	0.15	18.55	0.20	-0.32	18.67	0.70	2.559	2.379	2.272	2.172	2.066
1 15 44	2 42 20	136.1	-59.2	300.9	-4.8	0.672	17.50	* 0.20	17.70	0.20	-0.22	17.72	0.80	1.984	1.887	1.854	1.813	1.761
1 18 28	3 28 19	137.1	-58.3	301.8	-5.2	0.765	18.50	* 0.30	18.80	0.21	-0.14	18.73	1.13	1.860	1.754	1.716	1.671	1.614
1 22 56	0 21 34	140.7	-61.1	298.4	-7.4	1.070	16.70	0.28	16.98	0.21	-0.15	16.92	0.17	2.437	2.307	2.253	2.193	2.121
1 23 56	25 43 54	132.8	-36.2	323.5	0.0	2.360	17.50	* 0.10	17.60	0.26	-0.37	17.71	0.88	2.834	2.646	2.527	2.420	2.308
1 33 40	20 42 18	136.8	-40.7	319.4	-3.7	0.425	18.10	0.05	18.15	0.25	-0.21	18.11	0.99	1.636	1.566	1.546	1.519	1.482
1 52 25	43 32 0	135.0	-17.6	342.3	0.3	1.460	19.00	* 0.30	19.30	0.46	-0.26	19.10	0.85	2.213	2.060	1.986	1.909	1.822
1 55 14	-10 58 17	167.6	-66.4	290.0	-17.8	0.616	17.10	0.23	17.33	0.24	-0.28	17.37	0.89	2.000	1.908	1.878	1.841	1.792
2 2 10	31 57 18	140.6	-28.1	332.3	-5.8	1.466	18.00	* 0.30	18.30	0.33	-0.26	18.23	0.12	2.389	2.236	2.161	2.084	1.997
2 2 34	-17 15 37	186.4	-70.3	283.8	-20.8	1.740	18.00	* 0.30	18.30	0.24	-0.28	18.34	0.10	2.487	2.321	2.233	2.145	2.049
2 14 27	10 50 24	154.3	-46.5	313.3	-16.2	0.408	17.00	* 0.15	17.15	0.27	-0.19	17.07	0.83	1.821	1.753	1.734	1.708	1.673
2 25 35	-1 29 6	168.5	-55.0	301.8	-22.7	0.685	18.00	* 0.20	18.20	0.27	-0.21	18.14	0.80	1.911	1.812	1.778	1.737	1.684
2 32 36	-4 15 12	174.7	-56.3	299.4	-25.2	1.434	16.50	0.15	16.65	0.27	-0.26	16.64	0.88	2.693	2.541	2.468	2.392	2.306
2 33 0	-2 32 23	172.3	-54.4	301.3	-25.0	1.322	19.50	* 0.30	19.80	0.28	-0.17	19.69	0.70	2.025	1.880	1.813	1.741	1.659
3 17 57	-2 19 24	184.4	-46.5	305.2	-35.5	2.092	19.50	* 0.10	19.60	0.33	-0.32	19.59	0.84	2.369	2.190	2.084	1.985	1.879
3 33 22	32 8 37	159.0	-18.8	342.3	-22.5	1.263	18.50	* 0.30	18.80	0.62	-0.14	18.32	-0.11	2.269	2.127	2.063	1.994	1.915
3 36 59	-1 56 19	186.7	-41.7	307.6	-39.9	0.852	18.40	0.55	18.95	0.36	-0.16	18.75	0.19	1.924	1.811	1.768	1.718	1.656
3 49 10	-14 38 7	204.7	-46.1	291.7	-45.8	0.614	16.20	0.33	16.53	0.30	-0.28	16.51	1.17	2.170	2.078	2.048	2.011	1.962
3 50 4	-7 19 55	196.6	-42.7	301.9	-44.6	0.962	16.50	0.50	17.00	0.34	-0.16	16.82	1.00	2.389	2.267	2.218	2.163	2.096
4 3 14	-13 16 16	205.9	-42.7	294.4	-49.0	0.571	17.20	0.22	17.44	0.31	-0.29	17.42	0.78	1.946	1.859	1.831	1.796	1.750
4 5 27	-12 19 34	205.0	-41.8	295.9	-49.3	0.574	17.10	0.18	17.28	0.32	-0.29	17.25	0.71	1.983	1.895	1.867	1.832	1.786
4 14 49	-6 1 4	199.8	-37.1	306.3	-50.1	0.781	15.00	* 0.35	15.35	0.38	-0.16	15.13	2.01	2.594	2.487	2.448	2.402	2.344
4 20 43	-1 27 29	195.0	-33.0	313.7	-49.9	0.915	18.00	* 0.40	18.40	0.44	-0.17	18.13	-0.10	2.093	1.974	1.929	1.876	1.811

Simulations

Deriving the probability of a given anisotropy on purely mathematical grounds seems a very difficult problem because of an *a priori* anisotropic population density.

To by-pass this difficulty, we used a simulation process in agreement with our model (isotropic Gaussian HM*). We kept the supergalactic coordinates of the true 132 quasars to preserve the anisotropic distribution, but we assigned to each object a random Gaussian number instead of its own HM*. The standard deviation of these numbers was of course adjusted to agree with that of the real sample.

We constructed in this way 10 – artificial HM*, real position – samples and the search method was applied to them. For 6 out of the 10 simulations. we found an extremum of anisotropy larger than in the real sample. The probability that chance could cause the observed anisotropy is thus – in the frame of this *a priori* study – roughly 0.6. (We may note than an invalid use of the Student's test would give 0.13 only).

Our first conclusion is therefore that the hemispheric test of $\neg H'$ is negative: the observed anisotropy does not reach the 50% confidence level.

Now, are we able to give an upper limit for a possible hemispheric anisotropy of H_0? We reached a ΔHM* extremum of 0.1469 during the 10 simulations and this value was well separated from its challengers. So we may estimate at 0.9 the confidence level for chance not to generate ΔHM* higher than 0.147 (or 0.075 from mean).

The extremum deviation of the real sample from its mean is $\Delta'\mathrm{HM}^* = 0.052$. Therefore $0.052 + 0.075 = 0.127$ is an upper limit to the maximum deviation from isotropy which could be consistent with a true H_0 hemispheric anisotropy. If we take into account both the three-dimensional character of the addition of anisotropies and the rapidly decreasing distribution of the randomly generated Δ'HM*, we may give a lower limit 0.95 to the level of confidence of the foregoing result:

$\Delta'\mathrm{HM}^* \leqq 0.127$ $(t = 0.95)$.

This statement may be transposed to the Hubble constant through the expression of HM* and leads to upper limits for an hemispheric anisotropy of H_0 of $+34\%$ and -25% $(t = 0.95)$.

Smaller Scale Anisotropy

Real Sample

The method is slightly different. We defined a conical beam with an aperture 45°, 60° or 90°. The mean HM* was computed for objects which were lying inside the beam. This $\langle \mathrm{HM}^* \rangle_P$ was

Table 2 (continued)

b

1	2	3	4	5	6	7	8	9	10	11	12	13	14	15	16	17	18	19
4 21 33	1 57 21	192.0	-31.1	318.6	-48.7	0.689	17.50	* 0.20	17.70	0.47	-0.21	17.44	-0.24	2.055	1.956	1.922	1.880	1.827
7 10 15	11 51 30	204.8	10.1	35.9	-62.2	0.768	16.60	0.46	17.06	0.75	-0.17	16.48	1.03	2.313	2.207	2.168	2.123	2.065
7 25 20	14 43 47	203.8	14.6	42.0	-58.6	1.382	18.90	0.43	19.33	0.54	-0.23	19.02	0.84	2.190	2.042	1.971	1.897	1.813
7 29 20	81 52 36	132.1	28.5	28.0	7.6	1.022	17.50	* 0.40	17.90	0.47	-0.15	17.59	0.71	2.276	2.149	2.098	2.040	1.970
7 36 42	1 43 57	217.0	11.4	59.7	-69.5	0.191	17.50	0.43	17.93	0.64	-0.10	17.39	0.11	1.357	1.320	1.311	1.299	1.281
7 40 57	38 0 31	181.8	26.1	38.3	-35.2	1.063	17.60	0.45	18.05	0.36	-0.14	17.83	1.14	2.251	2.121	2.068	2.008	1.936
8 2 4	10 23 58	211.9	20.9	61.2	-58.8	1.952	18.40	0.25	18.65	0.38	-0.31	18.58	1.22	2.522	2.347	2.248	2.154	2.052
8 10 0	48 22 7	171.2	33.3	40.7	-23.7	0.871	17.80	0.57	18.37	0.30	-0.16	18.23	0.95	2.043	1.928	1.885	1.834	1.771
8 12 47	2 4 11	221.1	19.5	76.6	-63.4	0.402	18.50	* 0.15	18.65	0.39	-0.19	18.45	0.82	1.539	1.471	1.452	1.427	1.392
8 33 18	65 24 6	150.3	35.5	37.0	-6.8	1.112	18.20	0.55	18.75	0.33	-0.14	18.56	0.97	2.135	2.003	1.946	1.884	1.811
8 35 11	58 4 46	159.3	36.9	40.3	-13.3	1.534	17.60	0.49	18.09	0.30	-0.27	18.06	0.90	2.454	2.297	2.219	2.140	2.050
8 36 15	19 32 25	206.1	32.1	63.5	-46.6	1.691	17.60	0.0	17.60	0.27	-0.28	17.61	0.86	2.614	2.450	2.364	2.278	2.184
8 37 28	-12 3 54	237.6	17.1	112.1	-64.3	0.200	15.80	0.02	15.82	0.45	-0.11	15.48	0.93	1.759	1.721	1.712	1.699	1.680
8 38 2	13 23 6	213.0	30.1	70.0	-51.0	0.684	18.20	0.43	18.63	0.28	-0.21	18.56	0.75	1.826	1.728	1.694	1.653	1.600
8 43 1	13 39 57	213.2	31.4	71.1	-50.0	1.875	17.80	0.45	18.25	0.27	-0.28	18.26	0.80	2.557	2.385	2.290	2.198	2.098
8 46 58	10 0 32	217.6	30.7	76.3	-51.8	0.366	19.20	0.20	19.40	0.27	-0.17	19.30	1.08	1.316	1.254	1.236	1.213	1.181
8 50 23	14 4 17	213.7	33.2	72.6	-48.4	1.109	17.40	0.34	17.74	0.26	-0.14	17.62	1.17	2.322	2.189	2.133	2.071	1.998
8 56 4	17 3 8	211.0	35.6	70.9	-45.4	1.449	17.40	0.40	17.80	0.25	-0.26	17.81	0.91	2.465	2.312	2.239	2.162	2.076
9 3 44	16 58 16	211.9	37.2	72.8	-44.1	0.411	18.30	0.21	18.51	0.24	-0.20	18.47	0.90	1.546	1.478	1.458	1.433	1.397
9 22 22	14 57 26	216.5	40.6	78.9	-42.0	0.896	18.00	0.54	18.54	0.22	-0.17	18.49	1.03	2.010	1.893	1.848	1.796	1.732
9 22 36	0 32 6	232.5	33.8	96.6	-49.6	1.720	18.10	0.21	18.31	0.25	-0.28	18.34	-0.19	2.479	2.314	2.226	2.140	2.044
9 26 1	11 47 33	220.8	40.1	83.1	-43.2	1.754	19.10	0.12	19.22	0.22	-0.28	19.28	1.11	2.306	2.139	2.050	1.962	1.866
9 27 30	36 14 37	188.1	46.8	61.0	-26.5	1.157	18.20	* 0.40	18.60	0.22	-0.13	18.51	0.73	2.173	2.037	1.978	1.914	1.839
9 32 43	2 16 18	232.4	36.8	95.9	-46.6	0.659	17.40	0.13	17.53	0.24	-0.23	17.52	1.00	2.011	1.914	1.882	1.842	1.791
9 57 44	0 19 50	239.1	40.8	101.9	-41.6	0.907	17.60	0.47	18.07	0.22	-0.17	18.02	0.88	2.112	1.994	1.948	1.896	1.831
10 4 44	13 5 18	225.1	49.1	88.2	-34.5	0.240	15.20	0.13	15.33	0.20	-0.13	15.26	0.73	1.898	1.854	1.843	1.827	1.805
10 12 49	48 53 12	166.7	53.1	57.7	-11.8	0.385	19.00	* 0.15	19.15	0.22	-0.18	19.11	0.80	1.382	1.317	1.298	1.274	1.240
10 23 55	6 42 51	237.2	49.9	97.6	-33.1	1.699	18.30	0.54	18.84	0.20	-0.28	18.92	1.37	2.354	2.190	2.103	2.017	1.923
10 38 41	6 25 59	241.1	52.6	99.6	-29.9	1.270	16.80	0.16	16.96	0.20	-0.14	16.90	1.05	2.556	2.413	2.349	2.280	2.200
10 40 6	12 19 15	233.1	56.3	93.6	-27.2	1.029	17.30	0.46	17.76	0.19	-0.15	17.72	0.72	2.252	2.125	2.073	2.015	1.945
10 46 57	5 21 26	244.7	53.6	101.6	-28.4	1.115	18.90	0.24	19.14	0.20	-0.13	19.07	1.26	2.035	1.902	1.845	1.783	1.709

compared with $\langle HM^* \rangle_{132}$ the mean of the total sample. The difference $\Delta' HM^* = \langle HM^* \rangle_P - \langle HM^* \rangle_{132}$ was assigned to the position of the axis of the beam. Then the beam was moved to sweep the whole sky in steps of 10° in both SGL and SGB.

Positions and intensities of the extrema of anisotropy are summarized in Table 4.

Simulations

They were performed in the way applied above to the study of hemispheric anisotropy. When taking into account the number of objects in each beam, we found anisotropies with significances higher than that of the real sample for 9 out of the 10 simulations (aperture 90°).

Thus no smaller scale anisotropy was detected. The result of the test of $\neg H'$ is still negative. But the greater noise corresponding to the smaller number of quasars in each beam, more than compensates for the higher angular resolution. The limits on a possible anisotropy are much wider. Using the process that worked for hemispheric anisotropy, we may give an upper limit for resolution 90° only as: $H_0(+92\%, -43\%)$.

Correlation with the Geometry of the LSC

Observations

If we look at the directional features of the above analysis, we may make some further remarks.

The first striking phenomenon is well summarized in Table 4: extrema of anisotropy are lying at low SGB for all beam apertures.

Our scanning in 10° steps "avoided" the supergalactic plane since the steps were: −85°, …, −5°, +5°, …, +85°. We are interested in seeing what a scanning could show when the pole of partition is precisely on the supergalactic equator.

Rates of hemispheric, 90° and 45° anisotropies when the pole of partition is at SGB = 0° are shown in Fig. 4. This new scanning brings out an extremum of hemispheric anisotropy higher than that previously reached. The stronger minimum of ΔHM^* is located at SGB = 0° and SGL = 135° (point *M* in Fig. 1) with $\Delta HM^* = -0.1061$. The minimum of Fig. 4a is centred at SGL = 120°.

The centre of the LSC is generally assumed to lie in the vicinity of the Virgo cluster (SGB = −2° and SGL = 104°, point

Table 2 (continued)

C 1	2	3	4	5	6	7	8	9	10	11	12	13	14	15	16	17	18	19
10 47 49	9 41 48	239.0	56.4	97.1	-26.5	0.786	17.90	0.40	18.30	0.19	-0.16	18.27	1.21	1.970	1.862	1.823	1.777	1.718
10 48 47	24 4 0	213.2	62.8	83.2	-20.0	1.270	18.50	* 0.30	18.80	0.18	-0.14	18.76	1.11	2.185	2.043	1.978	1.909	1.829
10 49 0	-9 2 12	260.9	43.0	117.8	-31.9	0.344	16.80	0.06	16.86	0.24	-0.17	16.79	0.85	1.784	1.724	1.708	1.686	1.655
10 55 18	49 55 36	159.2	58.7	61.1	-5.6	2.390	19.50	* 0.10	19.60	0.21	-0.39	19.78	0.89	2.430	2.241	2.121	2.013	1.900
10 55 55	1 50 8	251.5	52.8	106.2	-27.5	0.890	18.00	* 0.45	18.45	0.20	-0.17	18.42	0.29	2.019	1.903	1.858	1.807	1.743
11 0 28	77 15 8	130.4	38.5	38.1	9.4	0.311	15.70	-0.02	15.68	0.35	-0.15	15.48	0.74	1.992	1.937	1.922	1.902	1.874
11 11 53	40 53 42	172.7	65.9	70.4	-7.7	0.734	18.00	0.15	18.15	0.19	-0.17	18.13	0.90	1.956	1.853	1.817	1.773	1.717
11 16 6	-46 17 50	286.8	13.3	161.3	-27.9	0.710	17.00	* 0.20	17.20	0.69	-0.19	16.70	0.82	2.220	2.119	2.084	2.041	1.987
11 16 21	12 51 7	242.3	63.9	96.9	-18.9	2.118	19.30	0.14	19.44	0.18	-0.32	19.58	0.77	2.381	2.201	2.094	1.994	1.887
11 27 36	-14 32 57	275.0	44.0	126.0	-24.0	1.187	16.90	0.27	17.17	0.25	-0.13	17.05	-0.03	2.482	2.345	2.284	2.219	2.142
11 30 24	10 40 17	251.3	65.1	100.3	-16.4	0.540	17.50	0.11	17.61	0.19	-0.29	17.71	0.74	1.854	1.770	1.744	1.711	1.667
11 32 16	30 22 2	198.4	73.0	81.8	-8.6	0.614	18.20	0.24	18.44	0.18	-0.28	18.54	0.73	1.765	1.674	1.644	1.606	1.557
11 36 39	-13 34 9	277.3	45.9	125.4	-21.6	0.554	17.80	* 0.15	17.95	0.25	-0.29	17.99	0.81	1.813	1.728	1.701	1.667	1.622
11 37 9	66 4 26	134.2	49.7	49.5	6.9	0.652	16.30	0.18	16.48	0.28	-0.24	16.44	0.83	2.220	2.125	2.093	2.053	2.002
11 48 10	0 7 15	272.3	59.1	112.4	-15.6	1.982	17.60	0.17	17.77	0.21	-0.31	17.87	-0.05	2.674	2.499	2.398	2.302	2.199
11 56 58	29 31 27	199.4	78.4	84.6	-4.0	0.729	15.60	* 0.30	15.90	0.18	-0.18	15.90	0.16	2.398	2.295	2.259	2.215	2.160
12 6 42	43 56 5	147.5	71.4	71.7	2.8	1.400	18.40	0.58	18.98	0.20	-0.25	19.03	0.92	2.198	2.048	1.977	1.902	1.818
12 18 4	33 59 50	166.3	80.6	81.8	1.7	1.519	18.60	0.19	18.79	0.19	-0.27	18.87	0.88	2.285	2.129	2.052	1.973	1.884
12 23 12	25 14 30	232.0	83.8	90.5	0.2	0.268	16.00	* 0.20	16.20	0.18	-0.13	16.15	1.22	1.779	1.730	1.718	1.701	1.675
12 32 59	-24 55 46	298.3	38.7	139.8	-10.9	0.355	17.20	0.36	17.56	0.28	-0.17	17.45	0.82	1.670	1.610	1.593	1.570	1.539
12 41 28	16 39 18	293.4	79.1	100.0	1.8	0.557	19.00	0.23	19.23	0.18	-0.29	19.34	0.96	1.548	1.462	1.435	1.401	1.356
12 53 36	-5 31 8	305.1	57.4	122.1	-1.3	0.536	17.80	0.26	18.06	0.21	-0.29	18.14	0.20	1.765	1.682	1.656	1.623	1.579
12 58 14	40 25 15	115.3	76.8	77.6	11.1	1.659	19.40	-0.13	19.27	0.21	-0.28	19.34	1.09	2.253	2.091	2.007	1.922	1.829
13 5 23	6 58 14	314.5	69.2	110.9	4.9	0.599	17.00	0.13	17.13	0.19	-0.30	17.24	0.91	2.011	1.921	1.892	1.855	1.807
13 17 5	0 34 12	318.3	62.3	118.9	5.7	0.890	17.30	0.52	17.82	0.21	-0.17	17.78	0.84	2.146	2.030	1.985	1.934	1.870
13 18 50	11 22 34	328.0	72.5	107.4	9.2	2.171	19.10	0.12	19.22	0.20	-0.32	19.34	0.71	2.447	2.265	2.155	2.053	1.945
13 27 23	-21 26 34	314.8	40.5	139.7	2.1	0.528	16.70	0.10	16.80	0.28	-0.29	16.81	0.79	2.021	1.938	1.913	1.880	1.837
13 32 17	55 15 48	110.2	61.1	63.0	18.4	0.249	16.00	* 0.20	16.20	0.24	-0.13	16.09	0.97	1.752	1.706	1.695	1.679	1.655
13 35 31	-6 11 57	323.1	54.3	125.7	8.5	0.625	17.70	0.14	17.84	0.23	-0.27	17.88	0.93	1.908	1.815	1.784	1.746	1.697
13 40 30	60 36 55	111.8	55.7	57.3	19.4	0.961	18.10	0.39	18.49	0.26	-0.16	18.39	0.89	2.074	1.952	1.904	1.848	1.781
13 55 58	-41 38 19	316.4	19.8	160.8	1.0	0.313	16.00	* 0.18	16.18	0.51	-0.15	15.82	0.80	1.928	1.873	1.858	1.839	1.810

V in Fig. 1). We are therefore recording a minimum of HM*:

(i) in the supergalactic equator (but with a poor resolution)

(ii) 15°–30° from the centre of LSC.

We may also notice the good isotropy (ΔHM* = 0.027) between the 2 supergalactic hemispheres (pole of partition at the North supergalactic pole).

Discussion

The first part of our study was an *a priori* investigation of the isotropy of H_0 without any other phenomenological hypothesis (i.e., we were looking at the intensity of a possible anisotropy, but without attention to its direction). We saw that no anisotropy reached the 50% confidence level in this frame.

We are now asking: "Is there a significant anisotropy?". The contradiction is apparent only and is removed by the distinction between "*a priori*" and "*a posteriori*" probabilities. If *a posteriori* we find that the direction of extremum anisotropy is in accordance with the consequences of some new plausible phenomenological hypothesis, we are then authorized to extend our investigation, because the significance of the former effect may be greatly increased by the addition of the directional parameter. Nevertheless, we are aware that conclusive tests of this new hypothesis will have to wait for new independent samples.

What new phenomenological hypothesis may we introduce in the frame of the former observations?

Figure 3c shows that a selection bias dependent on δ is unable to cause an hemispheric anisotropy of the order of 0.1 in HM*.

On the other hand, given the mean z of our sample (1.01) and the extremum of hemispheric anisotropy (ΔHM* = −0.1061), a solar motion solution would give an unrealistic $V_0 \sim 30{,}000$ km s^{-1}, an intensity conflicting with the isotropy of the 3 K background radiation (Smoot et al., 1977), even though the apices are close to each other (~30°).

Our extremum of hemispheric anisotropy (|ΔHM*| = 0.1061) is very much like that of Rubin-Ford (|ΔHM| = 0.11; Rubin et al., 1973), but the apices are almost antipodal (~150°) (Rubin et al., 1976).

In any case, explanations uncorrelated with the geometry of the LSC – or with its directional features – are hard to introduce *a posteriori* since we saw that they could reach the 50% confidence level only with difficulty.

Absorption by intergalactic matter in the disk of the LSC would be a possible hypothesis to account for our effect (HM* minimum through the centre and the disk). Our data would require an extinction ~0.5 mag through the disk. Coming back to our simulation process, we may give an estimation of the standard deviation for that measure ~0.5 mag. The supergalactic extinc-

Table 2 (continued)

d

1	2	3	4	5	6	7	8	9	10	11	12	13	14	15	16	17	18	19
14 16 39	6 42 21	352.2	60.7	115.7	22.0	1.439	16.80	0.33	17.13	0.26	-0.26	17.13	1.18	2.596	2.445	2.371	2.295	2.209
14 20 19	32 36 54	53.4	69.6	87.7	26.6	0.685	17.50	* 0.20	17.70	0.20	-0.21	17.71	0.18	1.996	1.897	1.864	1.823	1.770
14 21 15	-38 13 26	322.1	20.7	159.6	6.8	0.410	18.00	* 0.15	18.15	0.51	-0.20	17.84	0.74	1.670	1.601	1.582	1.556	1.520
14 42 50	10 11 12	5.8	58.2	113.6	29.1	3.530	17.80	0.73	18.53	0.29	0.29	17.95	-0.17	3.090	2.876	2.705	2.568	2.434
14 51 28	9 46 34	7.5	56.2	114.6	31.0	0.627	18.50	* 0.23	18.73	0.30	-0.27	18.70	0.26	1.745	1.652	1.622	1.584	1.534
14 53 12	-10 56 40	346.3	42.2	137.1	25.0	0.938	17.40	0.44	17.84	0.35	-0.16	17.65	0.77	2.207	2.087	2.040	1.986	1.920
14 54 3	-6 5 45	349.3	44.5	132.2	27.1	1.249	18.00	0.60	18.60	0.34	-0.14	18.40	0.70	2.245	2.104	2.041	1.973	1.893
15 10 9	-8 54 48	352.3	41.0	136.9	29.7	0.361	16.50	0.17	16.67	0.38	-0.17	16.46	-0.10	1.877	1.815	1.798	1.775	1.743
15 12 47	37 1 54	59.9	58.3	81.8	37.1	0.370	15.50	* 0.15	15.65	0.20	-0.18	15.63	0.78	2.056	1.993	1.976	1.952	1.919
15 45 31	21 1 34	33.9	49.5	102.5	45.4	0.264	16.70	0.11	16.81	0.29	-0.13	16.65	0.72	1.671	1.623	1.610	1.594	1.569
15 46 58	2 46 7	10.8	40.9	127.6	42.5	0.412	18.00	* 0.15	18.15	0.41	-0.20	17.94	-0.19	1.654	1.586	1.566	1.540	1.504
15 48 21	11 29 47	21.3	45.1	116.0	45.1	0.436	17.00	* 0.15	17.15	0.36	-0.22	17.01	0.80	1.871	1.800	1.779	1.752	1.714
16 11 48	34 20 20	55.2	46.4	81.8	49.4	1.401	17.50	* 0.30	17.80	0.24	-0.25	17.81	0.09	2.441	2.291	2.220	2.146	2.061
16 18 7	17 43 30	33.2	41.1	107.9	53.0	0.555	16.40	0.12	16.52	0.35	-0.29	16.46	0.93	2.121	2.035	2.008	1.974	1.929
16 22 33	23 52 1	41.4	42.1	97.5	53.8	0.927	17.50	0.44	17.94	0.31	-0.16	17.79	0.73	2.170	2.050	2.004	1.950	1.885
16 34 21	26 54 18	46.2	40.3	91.6	56.0	0.561	17.80	0.26	18.06	0.30	-0.29	18.05	0.72	1.808	1.722	1.695	1.661	1.615
16 41 18	39 54 11	63.5	41.0	69.9	52.5	0.594	16.00	0.29	16.29	0.24	-0.30	16.34	0.26	2.184	2.095	2.065	2.029	1.982
17 4 4	60 48 30	90.1	36.4	43.8	40.8	0.371	15.30	0.13	15.43	0.31	-0.17	15.29	0.73	2.126	2.063	2.045	2.022	1.989
18 1 44	1 1 18	28.4	11.0	164.8	70.7	1.522	19.00	* 0.25	19.25	1.41	-0.27	18.11	1.10	2.440	2.284	2.207	2.127	2.038
18 28 13	48 42 39	77.2	23.5	34.1	56.6	0.691	16.80	0.24	17.04	0.40	-0.20	16.84	0.75	2.177	2.078	2.044	2.002	1.949
19 54 23	51 23 46	85.3	11.8	11.1	52.2	1.230	18.50	* 0.30	18.80	0.91	-0.14	18.03	0.12	2.309	2.169	2.106	2.039	1.960
20 5 46	-4 27 18	38.2	-19.0	250.1	63.0	0.589	18.00	* 0.15	18.15	0.74	-0.30	17.71	1.11	1.906	1.817	1.788	1.752	1.705
20 59 9	3 29 49	52.7	-26.6	278.7	56.6	0.370	18.00	* 0.15	18.15	0.49	-0.17	17.83	-0.15	1.616	1.553	1.535	1.512	1.479
21 15 11	-30 31 50	16.3	-43.5	243.2	32.5	0.980	16.50	0.49	16.99	0.37	-0.15	16.77	0.72	2.411	2.287	2.238	2.182	2.114
21 20 26	16 51 46	67.9	-22.8	304.0	54.6	1.805	18.00	0.22	18.22	0.52	-0.28	17.98	0.98	2.585	2.417	2.325	2.235	2.137
21 28 53	-12 20 19	40.5	-40.9	263.0	42.3	0.501	16.00	0.13	16.13	0.36	-0.28	16.05	-0.15	2.142	2.063	2.039	2.008	1.966
21 35 1	-14 46 27	39.5	-43.0	261.5	39.7	0.200	15.50	0.10	15.60	0.34	-0.11	15.37	0.86	1.784	1.746	1.737	1.724	1.704
21 36 37	14 10 0	68.5	-27.5	300.2	50.4	2.429	18.50	* 0.20	18.70	0.44	-0.41	18.67	-0.03	2.663	2.473	2.351	2.241	2.128
21 45 36	6 43 43	63.7	-34.1	289.8	46.8	0.367	16.50	0.38	16.88	0.37	-0.17	16.68	0.05	1.841	1.779	1.761	1.738	1.706
21 46 46	-13 18 24	41.9	-45.3	265.1	38.1	1.800	20.00	* 0.20	20.20	0.32	-0.28	20.16	1.00	2.148	1.980	1.888	1.798	1.701
22 16 16	-3 50 43	60.2	-46.0	279.9	36.0	0.901	16.40	0.55	16.95	0.29	-0.17	16.83	0.86	2.345	2.227	2.182	2.130	2.066

e

1	2	3	4	5	6	7	8	9	10	11	12	13	14	15	16	17	18	19
22 30 8	11 28 23	77.4	-38.6	299.4	37.1	1.037	17.30	0.42	17.72	0.31	-0.15	17.56	0.06	2.290	2.163	2.110	2.052	1.981
22 49 8	18 32 47	87.4	-35.6	308.9	33.7	1.757	18.40	0.12	18.52	0.32	-0.28	18.48	0.70	2.466	2.299	2.210	2.121	2.02
22 51 30	15 52 54	86.1	-38.2	305.8	32.8	0.859	16.10	0.47	16.57	0.30	-0.16	16.43	0.08	2.395	2.281	2.238	2.188	2.12
22 51 41	11 20 39	82.8	-41.9	300.5	31.9	0.323	15.80	0.20	16.00	0.29	-0.16	15.87	0.77	1.933	1.876	1.861	1.841	1.811
22 52 35	12 57 34	84.3	-40.7	302.5	32.0	0.543	19.70	* 0.14	19.84	0.29	-0.29	19.84	0.78	1.432	1.348	1.322	1.288	1.244
22 54 44	2 27 18	75.8	-49.4	290.7	29.0	2.090	18.00	* 0.15	18.15	0.26	-0.32	18.21	-0.03	2.645	2.466	2.360	2.261	2.155
23 25 41	29 20 36	102.1	-29.9	322.2	26.3	1.015	17.30	0.65	17.95	0.33	-0.15	17.77	0.92	2.234	2.108	2.057	1.999	1.930
23 40 23	-3 40 20	86.1	-60.6	288.0	16.3	0.896	17.00	* 0.45	17.45	0.22	-0.17	17.40	0.70	2.228	2.111	2.066	2.014	1.950
23 44 3	9 14 4	97.5	-50.1	301.3	18.9	0.677	16.00	0.26	16.26	0.24	-0.22	16.24	0.15	2.283	2.185	2.152	2.111	2.059
23 53 28	-68 35 24	310.8	-48.5	227.7	-9.3	1.716	17.00	* 0.27	17.27	0.33	-0.28	17.22	0.24	2.703	2.538	2.450	2.364	2.269
23 54 45	14 29 26	103.9	-46.1	307.3	17.5	1.810	18.20	0.14	18.34	0.24	-0.28	18.38	0.75	2.507	2.338	2.246	2.156	2.059

Footnotes to Table 2

The following data are listed:

Col. 1 α_{1950} in h, min, s

Col. 2 δ_{1950} in d°, ′, ″

Col. 3 GL: Galactic Longitude in degrees and tenths, computed according to de Vaucouleurs et al. (1976), as for Col. 4, 5, 6

Col. 4 GB: Galactic Latitude

Col. 5 SGL: Supergalactic Longitude

Col. 6 SGB: Supergalactic Latitude

Col. 7 z: Emission redshift (Smith-Haeni, 1977)

Col. 8 V: V-magnitude (Smith-Haeni, 1977)

Col. 9 $B-V$: Colour index (Smith-Haeni, 1977; save for numbers marked with an asterisk, which are transcribed from the standard $B-V$ of Evans and Hart (1977) for the right z

Col. 10 B: B-magnitude from Col. 8 and 9

Col. 11 AB: Galactic B extinction, computed according to de Vaucouleurs et al. (1976), through the data in Col. 3 and 4

Table 2 (Footnote continued)

Col. 12 *KB*: *K*-correction for *B*-magnitude, after Evans and Hart (1977), when $z \leqq 2.5$, and from their transformation formula, when $z > 2.5$, as explained in the paragraph "corrections".
Col. 13 B0: *B*-magnitude corrected for colour, galactic extinction and *K*-correction
Col. 14 SPI: Radio spectral index between 408 and 1415 MHz after Smith-Haeni (1977)
Col. 15 HM* −1: Generalized Hubble modulus for the Hoyle model and computed from Col. 7 and 13, according to Eq. (3)
Col. 16 HM* 0: idem but for the Friedmann's model with $q_0 = 0$ and Eq. (3)
Col. 17 HM* 0.2: idem but for the Friedmann's model with $q_0 = 0.2$ and Eq. (3)
Col. 18 HM* 0.5: idem but for the Friedmann's model with $q_0 = 0.5$ and Eq. (3)
Col. 19 HM* 1: idem but for the Friedmann's model with $q_0 = 1$ and Eq. (3)

tion through a diameter of the LSC would then be: $A'_B = 0.5 \pm 0.5$ mag.

This latter part of our study is a blending of *a priori* and *a posteriori*. Classical tests of confidence are thus invalid. So it is for comparison only that we computed the Student's test for supergalactic absorption. If we put the pole of hemispheric partition on the Virgo cluster – which is not the position of the extremum anisotropy – the observed anisotropy leads to a Student's parameter 1.39. When looking at the consistent direction of the anisotropy (minimum through the centre of LSC) we should find that the probability of chance to cause the anisotropy is less than 0.08.

Because of the invalid use of the Student's test, we do not want to argue in any way that this is a proof of supergalactic extinction. Thus we only compare the above probability of chance with the one (0.60) of an H_0 anisotropy.

Actually, supergalactic extinction is not a new problem. Unpublished preliminary studies date from 1953 (de Vaucouleurs et al., 1972; de Vaucouleurs, 1977). Takase (1972) pointed out a 0.04 *B−V* colour excess through the centre of the LSC. This effect was confirmed by new measures (de Vaucouleurs et al., 1972) and leads to a total *B* extinction through the disk of the LSC, $A'_B = 0.24 \pm 0.08$, which is not inconsistent with our own figure. (See also Gross, 1977).

I was not aware of the former works on supergalactic extinction when I began my study. There lies the ethical reason why I cannot claim to have made an *a priori* statistical study.

However, supergalactic extinction has been later denied and colour excess imputed to intrinsic colours of galaxies in dense clusters (Abadi and Edmunds, 1975). De Vaucouleurs (1977) made a new study of this subject and did not find any *U−V* excess (the 1972 study showed *B−V* excess but not *U–B*).

Effect in Supergalactic Latitude (SGB)

We studied the variation of HM* versus SGB to test the hypothesis of extinction by the disk of the LSC in a new way. We divided the data into two hemispheres, one (*C*) pointing to the centre of the LSC (i.e., $14° < \mathrm{SGL} < 194°$) and the other (*A*) to the anticentre (i.e., $\mathrm{SGL} \leqq 14°$ or $\mathrm{SGL} \geqq 194°$). Each hemisphere has been divided into symmetric bands to SGB (i.e., bands of |SGB|).

For each band of |SGB| we computed the mean HM* in the *C* and *A* regions and the difference *C–A* (i.e., $\langle HM^* \rangle_C - \langle HM^* \rangle_A$). A crude division in 9 bands of 10° each would have supplied only 4 bands with high enough numbers of objects in each hemisphere.

Avoidance of the quick depletion of high latitude bands has been achieved by an equal area division. The equi-partition which gives steps ~10° at low latitudes is that which divides an hemi-

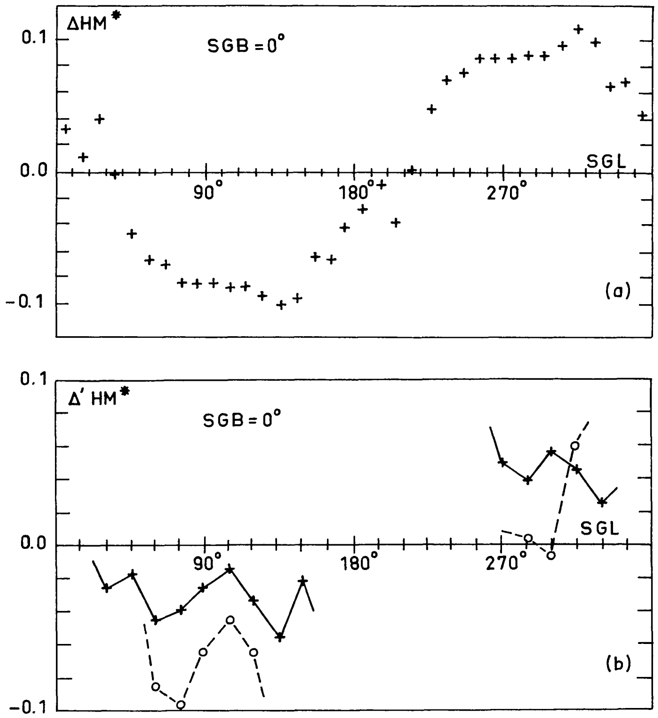

Fig. 4a and b. Anisotropy of HM* 0.5 along the supergalactic equator. **a** Hemispheric anisotropy of HM* (pole of partition at SGB = 0°) · $q_0 = 0.5$. The new minimum has been reported as *M* in Fig. 4. $\Delta HM^* = \langle HM^* \rangle_I - \langle HM^* \rangle_{II}$
b Smaller scale anisotropy of HM* along the supergalactic equator. $\Delta' HM^* = \langle HM^* \rangle_P - \langle HM^* \rangle_{132}$. Crosses show $\Delta' HM^*$ for an exploring beam *P* with a 90° aperture and a minimum of 15 objects in each beam. Open circles are for a 45° beam and a minimum of 8 objects

Table 3. Positions and intensities of extrema (minima) of hemispheric HM* for 5 rates of q_0. $\Delta HM^* = \langle HM^* \rangle_I - \langle HM^* \rangle_{II}$. SGL and SGB are the supergalactic coordinates of the centre of hemisphere I

q_0	SGL	SGB	ΔHM*
-1	135	+5	-0.1299
0	135	+5	-0.1174
0.2	135	+5	-0.1102
0.5	125	-25	-0.1051
1	125	-35	-0.0995

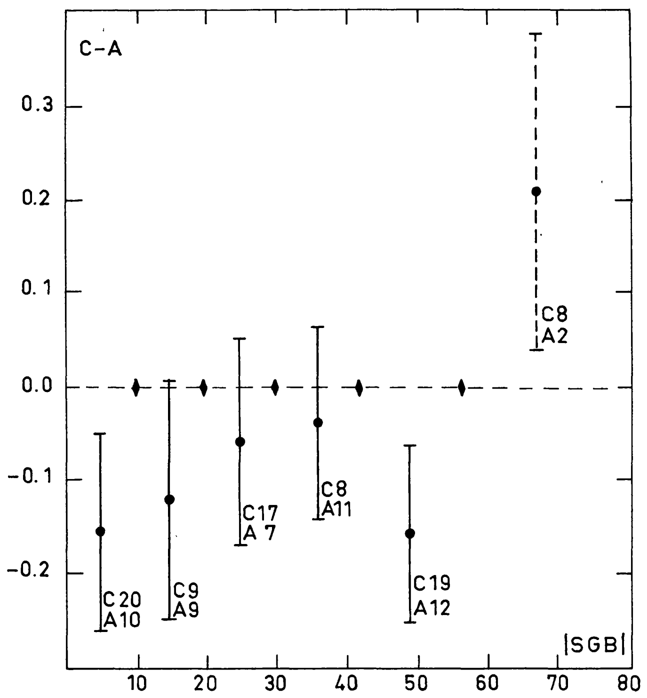

Fig. 5. Variation of HM* 0.5 versus |SGB|. *C–A* is the difference of ⟨HM*⟩ between the centre (*C*) and the anticentre (*A*) zones. Standard errors are figured for each mean value. The numbers of objects in the centre and the anticentre regions are indicated at the bottom of the error lines. The little lozenges on the zero dotted line show the limits of the 6 equal area bands of |SGB|

Table 4. Positions and intensities of extrema of Δ'HM* for several angular resolutions. $q_0=0.5$. ϕ_P is the aperture of the beam. N_m is the minimum number of objects in a beam which has been stated *a priori* before searching extrema (for the 180° study, this number appears *a posteriori*, since no selection has been set). SGL and SGB are the supergalactic coordinates of the centre of the beam. $\Delta'\mathrm{HM}^* = \langle \mathrm{HM}^* \rangle_P - \langle \mathrm{HM}^* \rangle_{132}$

ϕ_P	N_m	SGL	SGB	Δ'HM*
180º	(34)	305 125	+25 -25	+0.060 -0.045
90º	15	345 150	+30 -15	+0.105 -0.065
60º	10	335 145	+5 +5	+0.109 -0.125
45º	8	325 125	+15 -15	+0.127 -0.059

sphere into 6 bands of $2\pi/6$ steradians. Limits of the bands are then: |SGB| = 0°; 9°.59; 19°.47; 30°.00; 41°.81; 56°.44; 90°.00.

Figure 5 shows the variation of *C–A* versus |SGB|. An extinction effect by the disk of the LSC would be characterized by a negative minimum at |SGB| = 0°, followed by a growth towards *C–A* = 0 and then by a constant level at high |SGB|. Data are consistent with this feature, except for the point at SGB ~ 50°.

We have to note that this test is not entirely "*a priori*" [the first study had shown that HM* was minimum in the general directions of low |SGB| (< 30°) and *C* hemisphere]. Furthermore, standard errors in Fig. 5 show that data are also compatible with a zero |SGB| effect (constant *C–A*). Finally, under the extinction hypothesis, data in Fig. 5 would lead to $A'_B = 0.8 \pm 0.5$ mag through the diameter of the disk of the LSC which is too high compared with the findings of the above-mentioned works.

We may recall that an anti-correlation exists between galactic and supergalactic latitudes through the orthogonality of the two equators (Gula et al., 1975). This complicates the separation of a possible supergalactic extinction from residual errors in galactic extinction. A small sample of quasars is not capable of separating the two effects, but I think that in spite of the dispersion of the data, studies on new independent samples of objects well outside the LSC are a way to test:

(i) the reality of the observed anisotropy
(ii) its origin.

Conclusion

A sample of 132 quasars selected by their radio spectral index does not show significant departures from isotropy of a generalized Hubble modulus HM* (hence of H_0) for angular resolutions 180°, 90°, 60°, and 45°. An upper limit for a possible hemispheric anisotropy at very large distances is H_0 (−25%, +34%).

Nevertheless, the observed anisotropy is near the 50% level of confidence without any consideration of its direction. Moreover, HM* is minimum in the general direction of the centre of the LSC. A minimum of HM* is a lack of redshift or an excess of magnitude. The former is too large (~3 10^4 km s^{-1}) to be explained by solar motion. The hypothesis of a supergalactic extinction which could cause the latter is not ruled out by the study of the dependence of HM* on the supergalactic latitude, but the intensity of extinction ($A'_B = 0.8 \pm 0.5$ mag through a diameter of the LSC) is too large compared with earlier studies. This, combined with the large dispersion of the data, requires that the present conclusion merely poses the possibility of the supergalactic extinction. Further investigation of the causes of the HM* anisotropy needs preliminary tests of its reality on new samples.

Acknowledgements. It is a great pleasure to thank my supervisor Prof. H. Andrillat for many discussions, counsels and improvements. My thanks also go to Mrs M. O. Mennessier, who suggested the use of simulation process. In addition, I am indebted to J. P. Cordoni for his contribution to the programming of the statistical study and to P. Boissé who made me acquainted with previous works on supergalactic extinction. Finally, I wish to thank Prof. G. de Vaucouleurs for critically reading several earlier versions of this paper and making many helpful suggestions.

References

Abadi, H.I., Edmunds, M.G.: 1975, *Astron. Astrophys.* **45**, 319
Cordoni, J.P., Reboul, H.: 1979, *Compt. Rend. Acad. Sci. Paris* **288**, B139
de Vaucouleurs, G.: 1958, *Astron. J.* **63**, 254
de Vaucouleurs, G.: 1964, *Astron. J.* **69**, 737
de Vaucouleurs, G.: 1976, *Astrophys. J.* **205**, 13

de Vaucouleurs, G.: 1977, in *The Large Scale Structure of the Universe*, M. S. Longair and J. Einasto (eds.), p. 205
de Vaucleurs, G., de Vaucouleurs, A., Corwin, H.G.Jr.: 1972, *Astron. J.* **77**, 285
de Vaucouleurs, G., de Vaucouleurs, A., Corwin, H.G.Jr.: 1976, in *Second Reference Catalogue of Bright Galaxies*, University of Texas Press
de Vaucouleurs, G., Peters, W.L.: 1968, *Nature* **220**, 868
de Vaucouleurs, G., Bollinger, G.: 1979, *Astrophys. J.* **233**, 433
Evans, A., Hart, D.: 1977, *Astron. Astrophys.* **58**, 241
Gross, P.G.: 1977, *Astrophys. J.* **215**, 417
Gula, R., Rudnicki, K., Tarraro, I.: 1975, *Acta Cosmol.* **315**, 3, 39
Jaakola, T., Karoji, H., Moles, M., Vigier, J.P.: 1975, *Nature* **256**, 25
Jaakola, T., Karoji, H., Le Denmat, G., Moles, M., Nottale, L., Vigier, J.P., Pecker, J.C.: 1976, *Monthly Notices Roy. Astron. Soc.* **177**, 191
Karoji, H., Moles, M.: 1975, *Compl. Rend. Acad. Sci. Paris* **280**, B 609
Karoji, H., Nottale, L., Vigier, J.P.: 1975a, *Astrophys. Space Sci.* **44**, 229; 1975b, *Compl. Rend. Acad. Sci. Paris* **281**, B409
Karoji, H., Nottale, L.: 1976, *Nature* **259**, 31
Le Denmat, G., Vigier, J.P.: 1975, *Compl. Rend. Acad. Sci. Paris* **280**, B459
Nottale, L.: 1976, *Compl. Rend. Acad. Sci. Paris* **282**, 519
Nottale, L., Vigier, J.P.: 1977, *Nature* **268**, 608
Rubin, V.C.: 1951, *Astron. J.* **56**, 47
Rubin, V.C., Ford, W.K.Jr., Rubin, J.S.: 1973, *Astrophys. J.* **183**, L111
Rubin, V.C., Thonnard, N., Ford, W.K.Jr., Roberts, M.S.: 1976, *Astron. J.* **81**, 719
Setti, G., Woltjer, L.: 1973a, *Ann. New-York Acad. Sci.* **224**, 8
Setti, G., Woltjer, L.: 1973b, *Astrophys. J.* **181**, L61
Smith-Haeni, A.L.: 1977, *Astron. Astrophys. Suppl. Ser.* **27**, 205
Smoot, G.F., Gorenstein, M.V., Muller, R.A.: 1977, *Phys. Rev. Letters* **39**, 898
Stannard, D.: 1973, *Nature* **246**, 295
Takase, B.: 1972, *Publ. Astron. Soc. Japan* **24**, 295